coatings

MDPI

Article

Strong Radiative Cooling Coating Containing In Situ Grown TiO_2/CNT Hybrids and Polyacrylic Acid Matrix

Jiaziyi Wang [1], Yong Liu [2], Dapeng Liu [2], Yong Mu [2] and Xilai Jia [1,*]

[1] School of Materials Science and Engineering, University of Science and Technology Beijing, Beijing 100083, China
[2] Tangshan Power Supply Company, State Grid Jibei Electric Power Co., Ltd., Tangshan 063000, China
* Correspondence: jiaxl@ustb.edu.cn

Abstract

Traditional forced-air cooling systems suffer from excessive energy consumption and noise pollution. This study proposes an innovative passive cooling strategy through developing aqueous radiative cooling coatings made from a combination of TiO_2-decorated carbon nanotube (TiO_2-CNT) hybrids and polyacrylic acid (PAA), designed to simultaneously enhance the heat dissipation and improve the mechanical strength of the coating films. Based on CNTs' exceptional thermal conductivity and record-high infrared emissivity, bead-like TiO_2-CNT architectures have been prepared as the filler in PAA. The TiO_2 nanoparticles were in situ grown on CNTs, forming a rough surface that can produce asperity contacts and enhance the strength of the TiO_2-CNT/PAA composite. Moreover, this composite enhanced heat dissipation and achieved remarkable cooling efficiency at a small fraction of the filler (0.1 wt%). The optimized coating demonstrated a temperature reduction of 23.8 °C at an operation temperature of 180.7 °C, coupled with obvious mechanical reinforcement (tensile strength from 13.7 MPa of pure PAA to 17.1 MPa). This work achieves the combination of CNT and TiO_2 nanoparticles for strong radiative cooling coating, important for energy-efficient thermal management.

Keywords: carbon nanotube; radiative cooling; nanocomposite coating; thermal management

check for updates

Academic Editor: Gianfranco Carotenuto

Received: 30 May 2025
Revised: 22 July 2025
Accepted: 23 July 2025
Published: 7 August 2025

Citation: Wang, J.; Liu, Y.; Liu, D.; Mu, Y.; Jia, X. Strong Radiative Cooling Coating Containing In Situ Grown TiO_2/CNT Hybrids and Polyacrylic Acid Matrix. *Coatings* **2025**, *15*, 921. https://doi.org/10.3390/coatings15080921

Copyright: © 2025 by the authors. Licensee MDPI, Basel, Switzerland. This article is an open access article distributed under the terms and conditions of the Creative Commons Attribution (CC BY) license (https://creativecommons.org/licenses/by/4.0/).

1. Introduction

Efficient and energy-saving heat dissipation is extremely important in the face of huge energy consumption. Traditional forced-air cooling systems suffer from excessive energy consumption and noise pollution [1]. This method is mainly used in large-size devices, such as box-type substations. With the continuous expansion of power supply capacity, radiative cooling should be very effective because the radiation transfer of energy requires no additional space and, more importantly, is independent of the surrounding conditions [2–4].

In various cooling techniques, radiative cooling methods have been reported based on various coating layers since it is very energy-saving and could be easily coated on various substrates [5–7]. Among these, aluminum has emerged as the material of choice for electronic applications owing to their exceptional moisture barrier properties and corrosion resistance. To achieve better radiative cooling effects, various fillers with carefully designed micro- or nano-structures are used in the development of efficient radiation heat dissipation layers [8–13]. However, the existing matrix used for radiative cooling materials is generally

a polymeric material. The strength of the polymeric coating is easy to be damaged by external forces; in addition, the coating layers are gradually aged under light.

Carbon nanotubes (CNTs) have a high infrared emissivity and are one of the most radiant materials at present [14–16]. They can effectively absorb heat from the environment and emit it in the form of infrared radiation, thus achieving the effect of heat dissipation [17–19]. On the other hand, titanium dioxide (TiO_2) can produce high reflectivity in the solar radiation band [20]. For example, the radiative cooling material composed of polydimethylsiloxane and TiO_2 spheres can achieve good thermal dissipation and reduce energy consumption for cooling [21].

Prashantha et al. [22] prepared multi-wall carbon nanotubes (MWCNTs)/Polypropylene (PP) nanocomposites by diluting a MWCNTs/PP masterbatch by melt compounding with a twin screw extruder. An increase of 17.73% in tensile strength was observed for the 1 wt% MWCNTs/PP composite relative to the pure PP matrix. Safadi et al. [23] fabricated MWCNTs/PS composite by the film casting of polystyrene (PS) incorporated with MWCNTs, resulting in a 25.64% enhancement in tensile strength relative to neat PS at 1 wt% MWCNTs loading. Suryawanshi et al. [24] prepared molecular fan (MF) coatings by dispersing MWCNTs into an acrylate (AC) emulsion at various loadings (0 wt%, 0.4 wt%, 0.7 wt%, and 1.0 wt%). At an operating temperature of 87 °C, it was observed that increasing the MWCNTs content resulted in an equilibrium temperature cooling efficiency of 8.04%, 10.34%, 16.09%, and 19.54% for the pure AC, 0.4 wt%, 0.7 wt%, and 1.0 wt% composite coatings, respectively. Considering the advantages of CNTs and TiO_2, it is aimed to combine the two together for better radiative cooling materials. The carboxyl groups (–COOH) within the molecular structure of polyacrylic acid (PAA) can form stable ionic bonds with metal ions, such as Al^{3+}, Cu^{2+}, and Fe^{3+}. This bonding mechanism enhances the interfacial adhesion between the PAA coating and the substrate [25]. The resulting improvement in interfacial integrity significantly inhibits the permeation of water molecules, thereby effectively preventing the initiation of corrosion reactions. This study proposes an innovative passive cooling strategy through developing aqueous radiative cooling coatings made from a combination of TiO_2-decorated carbon nanotube (TiO_2-CNT) hybrids and PAA. Based on CNTs' exceptional thermal conductivity and record-high infrared emissivity, bead-like TiO_2-CNT architectures have been prepared as the filler in PAA matrix. The TiO_2 nanoparticles were in situ grown on CNTs, forming a rough surface that can produce asperity contacts and enhance the strength of the TiO_2-CNT/PAA composite. Moreover, this composite synergistically enhances heat dissipation while maintaining antistatic performance, achieving remarkable cooling efficiency. This work achieves the combination of CNT and TiO_2 nanoparticles for strong radiative cooling coating, important for energy-efficient thermal management.

2. Materials and Methods

2.1. Synthesis of TiO_2-CNT Hybrid Material

Based on our previous work [26], 100 g of the HNO_3-oxidized CNTs was dispersed into 2.5 L of 5.0 wt% tetrabutyl titanate–ethanol solution. The mixture was stirred for 1.5 h with a magnetic stirrer. After that, the CNTs were washed with ethanol, filtered, and dried to form the tetrabutyl-titanate-modified CNTs. Then, 2.0 g of tetrabutyl-titanate-modified CNTs was thermally treated in a tube furnace under an air atmosphere at 450 °C for 2 h, with a heating rate of 5 °C min^{-1} to form a bead-like TiO_2-CNT structure for use.

2.2. In Situ Polymerization of TiO_2-CNT/PAA Composites

To make CNT dispersion, 0.18 g, 0.54 g, and 0.9 g of TiO_2-CNT and 135 mL of deionized water were mechanically dispersed in a homogenizer (5000 rpm, 50 min), respectively. After

that, 0.0315 g of potassium persulfate initiator was added to 15 mL of water and stirred at 600 rpm for 30 min to prepare initiator solution. After that, 30 mL of acrylic acid monomer and 135 mL of CNT dispersions at varying mass concentrations were mixed in a 250 mL three-neck flask, and purged with nitrogen to eliminate oxygen. The mixture was heated to 80 °C while stirring at 200 rpm. The initiator solution was added dropwise within 8 min. The in situ polymerization process was carried out at 80 °C under the stirring speed of 500 rpm for 4 h, resulting in homogeneous TiO_2-CNT/PAA composite paints. The as-prepared TiO_2-CNT/PAA paints were subjected to vacuum extraction and then cast into polytetrafluoroethylene (PTFE) molds. The samples were dried at 50 °C for 8 h, producing homogeneous films with approximate thickness of 0.4 mm for morphological and mechanical characterization. To make coated specimens on Al substrates, two sequentially cured coatings (60 μm thick each) were deposited onto high-purity aluminum substrates (30 mm × 30 mm, 250 μm thick) using an adjustable film applicator, dried at 50 °C for 30 min, yielding a final dry thickness of approximately 370 μm. The corresponding nanocomposites were TiO_2-CNT/PAA of 0.1 wt%, 0.3 wt%, and 0.5 wt%, respectively, based on the mass calculation.

2.3. Characterizations

Thermogravimetric analysis (TGA) was performed using a TGA/DSC 1/1600LF from Mettler Toled (Greifensee, Switzerland) under air atmosphere. Samples were heated from room temperature to 800 °C in Al_2O_3 crucibles at a heating rate of 5 °C min^{-1}. DSC measurements were conducted under nitrogen flow from room temperature to 300 °C in Al_2O_3 crucibles at a heating rate of 10 °C min^{-1}. X-ray Diffraction (XRD) patterns were acquired on a D8 ADVANCE diffractometer from Bruker (Karlsruhe, Germany) with Cu Kα radiation (λ = 1.5406 Å). Scans were performed over a 2θ range of 5–90° at a rate of 5° min^{-1}. Transmission electron microscopy (TEM) was conducted on a JEOL JEM2010 (Tokyo, Japan) at an accelerating voltage of 120 kV. Surface morphology was characterized by scanning electron microscopy (SEM) using a JSM7401 from JEOL (Tokyo, Japan) at 3.0 kV. Raman spectra were collected on a LabRAM HR800 spectrometer from HORIBA (Villeneuve-d'Ascq, France) with a 633 nm excitation laser. Adhesion tests were conducted according to Chinese National Standard GB/T 9286-2021 [27]. Successive sweeps were performed several times along each diagonal of the grid pattern using a soft-bristled brush. Tensile properties were evaluated using a WDW-5 universal testing machine from DOCER (Jinan, China). Dumbbell-shaped specimens were prepared for tensile stress test at a speed of 2 mm·min^{-1}. Surface temperatures of the Al sheet were recorded using a TM902C high-speed digital thermometer from Suohuan (Taizhou, China); range: −50–1300 °C, accuracy: ±1 °C or 0.75% of reading, while the temperatures of the coating surfaces were monitored by WIFI Thermocam infrared (IR) thermal imager from Beiqian Electronics (Dalian, China).

Thermal Radiation Evaluation Apparatus: To focus on thermal radiation effects, experiments were conducted in a corrugated cardboard chamber sealed with polyethylene film to eliminate convective/conductive heat transfer. High-purity aluminum sheets (30 × 30 mm^2), simulating substation enclosures, were bonded to a heating stage (system temperature: 200 °C) by applying thermal grease to their bottom surfaces. A silicone thermal pad, with a diameter of 0.8 cm and a thickness of 0.2 cm, was applied to the top surface of the aluminum panel and connected to a high-speed digital thermometer to measure the panel's temperatures. The temperatures of the coated aluminum panel surfaces were measured by an IR thermal imager located directly above the sample surface; thermal images were captured once per second. To account for the intrinsic thermal resistance of the silicone pad and thus normalize the measurement conditions, an identically sized pad was applied at the geometric center of every sample surface.

3. Results and Discussion

As we all know, TiO_2 has been widely used in coating paints, while CNTs can reduce the aging of the polymeric coating layers. To combine those advantages, tetrabutyl titanate molecules were first grafted onto the surfaces of the CNTs based on solution method [26]. After being oxidized in air at 450 °C for 2 h, the tetrabutyl titanate was converted into TiO_2 while the structure of the CNTs was maintained. This step formed the hybrids with nano TiO_2 attached on the CNT surfaces. This conversion results in the composite hybrids containing 12 wt% TiO_2 and 88 wt% CNTs, as displayed by TGA characterization (Figure 1a). The XRD pattern of the hybrids displayed sharp peaks of MWCNTs (26.3° (002) and 43.2° (400) peak, respectively) and very weak peaks of TiO_2 (Figure 1b). The reason for the weak intensity of the TiO_2 peaks is due to the very small size of the TiO_2 nanoparticles as observed under TEM. As shown in Figure 1c, the TiO_2 nanoparticles were well grown on the surface of the CNTs, with size distributing around 4–5 nm. The very small TiO_2 nanoparticles resulted in rough surfaces on the CNTs, effective for load transfer for their composites. Even though the XRD peaks of the TiO_2 was not obvious due to the small size, the high-resolution TEM figure of the hybrids displays typical lattice lines of the TiO_2 nanoparticles (Figure 1d), suggesting the successful preparation of the aimed TiO_2-CNT hybrids.

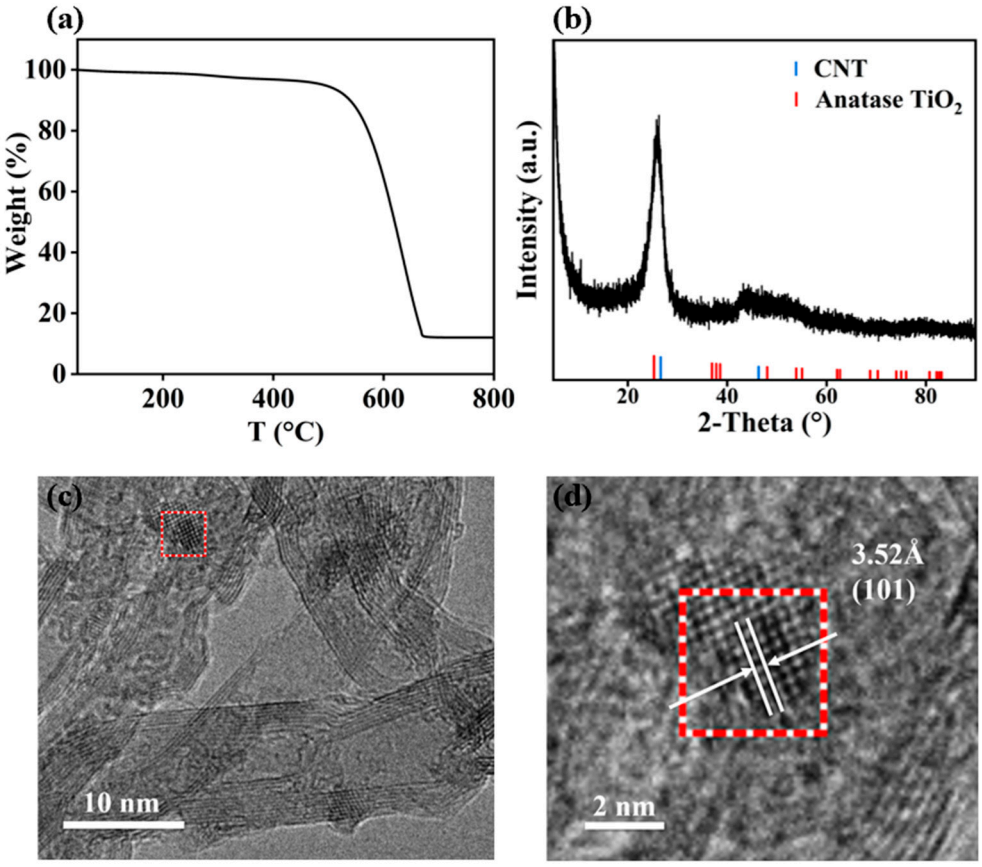


Figure 1. (**a**) TGA curve of the TiO_2-CNT hybrids in the air atmosphere, (**b**) XRD pattern of the TiO_2-CNT hybrids, (**c**,**d**) TEM images of the TiO_2-CNT hybrids with typical lattice lines.

The TiO_2-CNT hybrids can be well dispersed in aqueous PAA solution, since the PAA has carboxyl groups that can interact with TiO_2. Figure 2a shows the optical photograph of the TiO_2-CNTs hybrids dispersed in the PAA solution (0.3 wt%). It can be seen that no obvious phase separation occurred after standing for 12 h. When the TiO_2-CNT/PAA dispersion is coated on the substrates such as the Al sheets, uniform coating films can

be formed after drying. As the coating films, they should be strong and have robust adhesion to the substrates. In this case, the coated films were made a slit. As can be seen in Figure 2b–d, the composite coatings were not damaged except where the scratches were loaded. Those results support good adhesion of the TiO_2-CNT/PAA composites to the Al sheet, important for the surface integrity of coatings on electronic enclosures. Moreover, due to the anti-electrostatic properties, the composite film can be expected for better anti-aging.

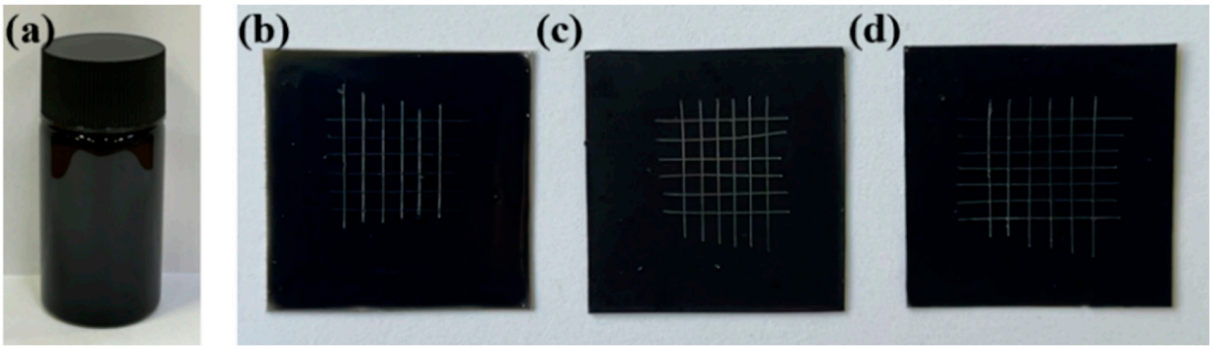


Figure 2. (**a**) Optical photograph of the TiO_2-CNTs hybrids dispersed in the PAA solution after standing for 12 h. Optical photographs of the coated films of TiO_2-CNT/PAA with scratches, (**b**) 0.1 wt%, (**c**) 0.3 wt%, and (**d**) 0.5 wt%.

Figure 3a compares the Raman shifts of the TiO_2-CNT filler and TiO_2-CNT/PAA composites. According to the comparison, the ratio of the D peak to the G peak (I_D/I_G) of the TiO_2-CNT/PAA composites is comparable to that of the CNTs. This indicates that the in situ polymerization causes no great damage to the CNTs. Good retention of the structural integrity of the CNTs is beneficial to maintaining their good mechanical strength and heat dissipation emissivity. Additionally, with the addition of PAA, the Raman shift moves to higher wave numbers, indicating that there are interactions between TiO_2-CNT and the PAA matrix [28,29]. This tight interaction helps to enhance the strength of the composite coating layers and enhance its heat dissipation ability. To investigate the effect of the introduction of TiO_2-CNTs, Figure 3b further compares the DSC melting curves of the nanocomposites with the PAA. The melting peak temperature of the composites shows a little decrease with increasing TiO_2-CNT content. This may be because the introduction of TiO_2-CNT filler causes reduced polymer molecular weight as displayed in the previous literature [30].

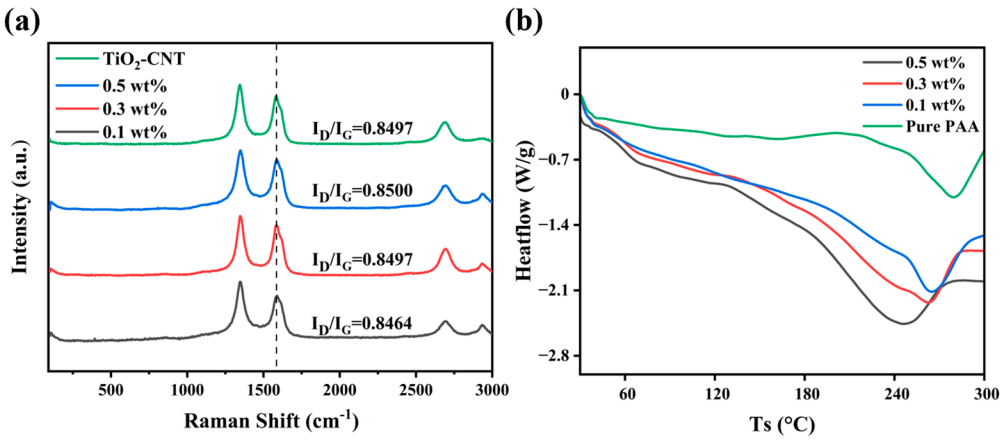


Figure 3. (**a**) Raman spectra for the TiO_2-CNT and TiO_2-CNT/PAA composites, (**b**) DSC curves of the PAA and TiO_2-CNT/PAA composites.

Broken cross-sections of the composites adding different ratios of TiO_2-CNTs were characterized by SEM (Figure 4). The surface of broken cross-section was very rough, and the cross-section was uniformly cracked for the 0.1 wt% (Figure 4a) and 0.3 wt% (Figure 4b) composite, while a relative aggregation of TiO_2-CNT hybrids was observed at a local region for the 0.5 wt% (Figure 4c,d) composite coating film. Figure 4e,f display TEM images of the 0.1 wt% TiO_2-CNT/PAA composite. As can be seen, the TiO_2-CNT hybrids were tightly wrapped by the PAA matrix, supporting good interfacial contact. The TiO_2 nanoparticles on the CNT surfaces might serve as the interlocks that enhanced the interaction of the CNTs with the PAA matrix, helpful to prevent CNTs from slipping out of the PAA matrix under stretching [31,32]. In this case, the load on the PAA matrix was effectively transferred onto the CNTs, which can provide an increased tensile strength as shown below.

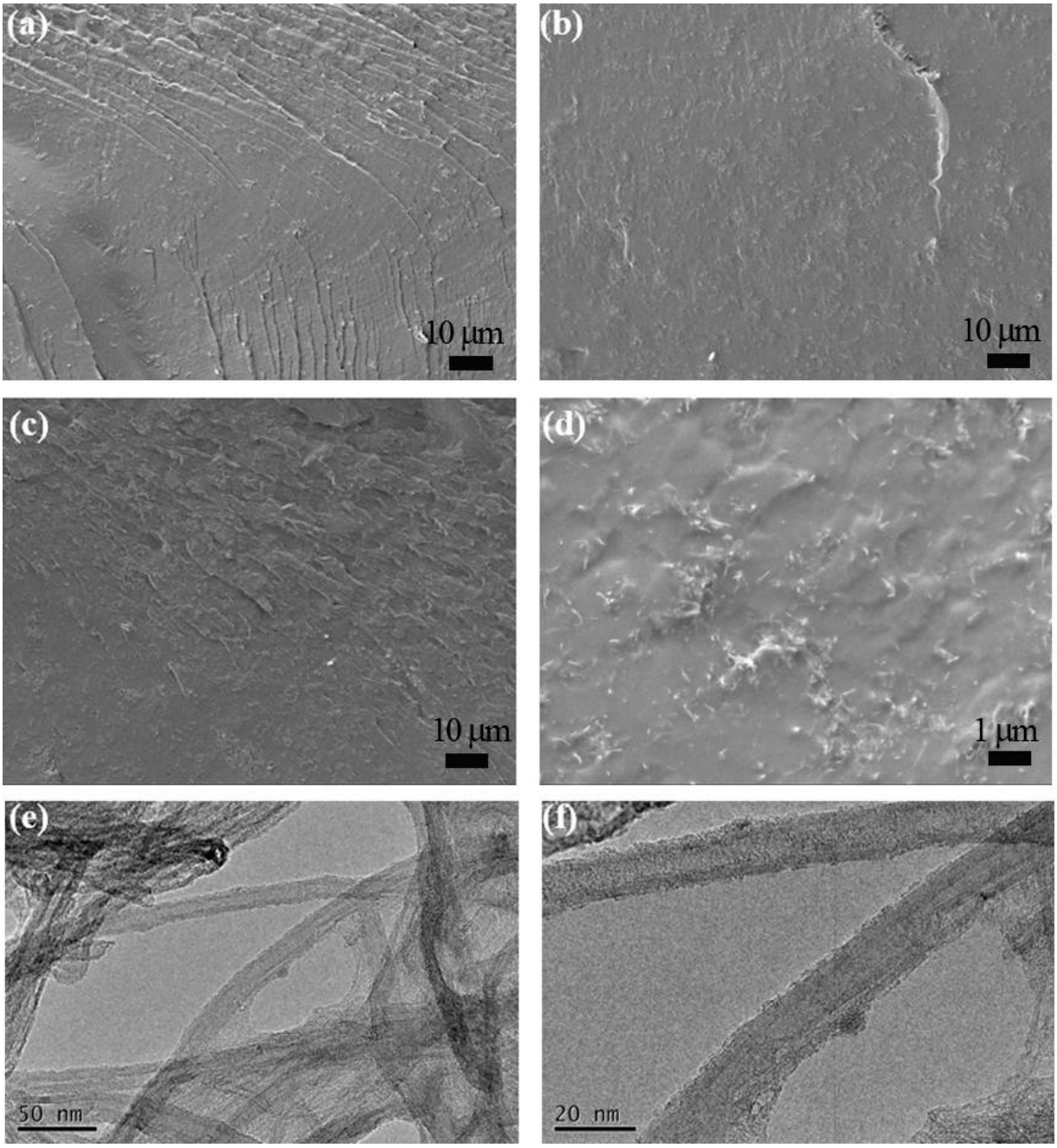


Figure 4. SEM images of the TiO_2-CNT/PAA composite coatings with (**a**) 0.1 wt%, (**b**) 0.3 wt%, and (**c**,**d**) 0.5 wt% TiO_2-CNT hybrid. (**e**,**f**) TEM images of the 0.1 wt% TiO_2-CNT/PAA composite.

Figure 5a shows that the as-prepared coating films can be tailored for strength testing. The composite coating films show good mechanical properties using PAA as the matrix. In Figure 5b, stress–strain curves of the TiO_2-CNT/PAA composite films are compared with that of pure PAA. The addition of 0.1 wt% TiO_2-CNT hybrids to the PAA matrix resulted in a composite whose strength at break shows an obvious increase, while its elongation shows very little increase. As the TiO_2-CNT hybrids were further increased to 0.3 wt%, the stress significantly increased to 28.9 MPa as compared to the pure PAA at a 13.7 MPa, even though the elongation decreased by half. With a further increase of the hybrids filler to 0.5 wt%, its elongation slightly increased, but its strength decreased to 18.4 MPa, which will eventually decrease its toughness. Stress toughness (Figure 5c) of the nanocomposites were also compared with the pure PAA. By increasing the hybrids filler, the stress toughness of the nanocomposites were 50.8 MJ m^{-3}, 30.2 MJ m^{-3}, and 26.2 MJ m^{-3} for the 0.1 wt%, 0.3 wt%, and 0.5 wt% TiO_2-CNT/PAA composites, respectively, compared to 33.3 MJ m^{-3} for the pure PAA. The 0.1 wt% and 0.3 wt% hybrids composite coating films have good mechanical properties in comparative aspects. The TiO_2 nanoparticles were in situ grown on CNTs, forming a rough surface that can produce asperity contacts and enhance the strength of the TiO_2-CNT/PAA composite.

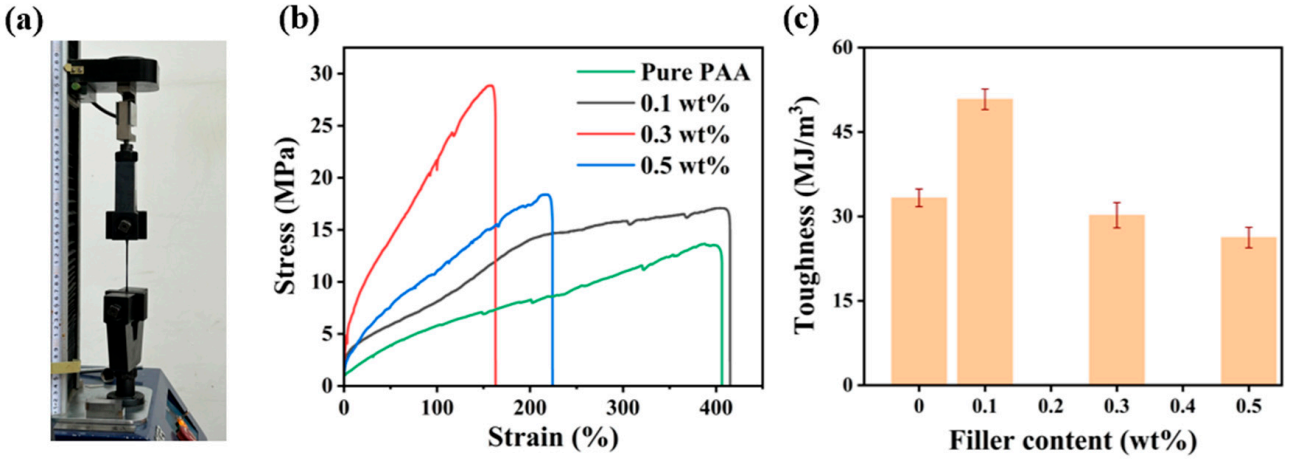


Figure 5. (**a**) Schematic diagram of tensile test of TiO_2-CNT composite film, (**b**) The stress–strain curves, (**c**) stress toughness of TiO_2-CNT/ PAA composite coating films.

Figure 6a compares the temperature vs. operation time profile of a bare aluminum control panel and aluminum panels with TiO_2-CNT/PAA coatings containing 0 wt% (pure PAA), 0.1 wt%, 0.3 wt%, and 0.5 wt% TiO_2-CNT hybrids. The uncoated aluminum panel was set as the control (black curve), whose surface temperature was tested by a high-speed digital thermometer. The temperatures of the coating surfaces were measured by the infrared thermal imager. The lowering of the equilibrium temperature for coated panels was measured relative to the uncoated panel. The largest temperature difference reached 23.8 °C for the 0.1 wt% TiO_2-CNT/PAA coatings (Figure 6b). The reason for the good cooling effect can be ascribed to the combination of high surface emissivity of MWCNTs and the high thermal conductivity. These results support that the as-designed TiO_2-CNT/PAA composite can efficiently emit absorbed heat as infrared radiation to the external environment, achieving good heat dissipation.

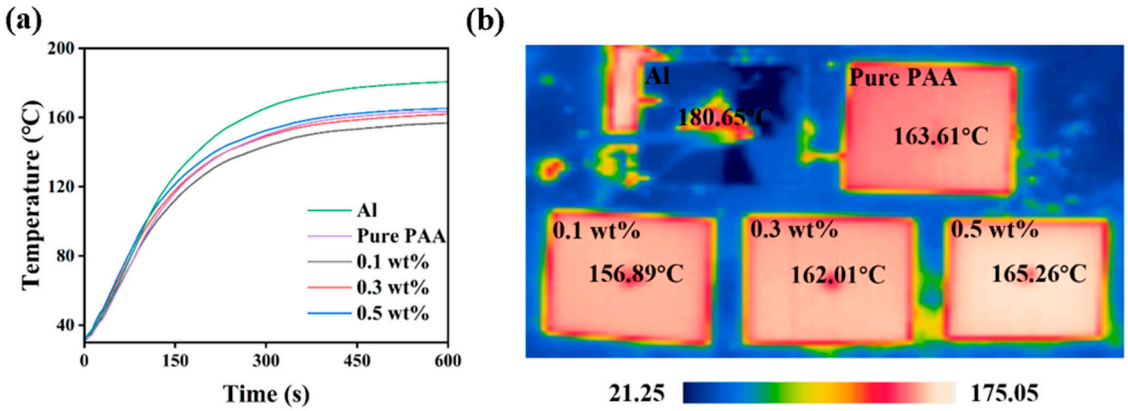


Figure 6. (**a**) Temperature vs. time curves and (**b**) infrared thermal image at 10 min for a bare aluminum control panel, and TiO_2-CNT/PAA composite coatings with 0 wt%, 0.1 wt%, 0.3 wt%, and 0.5 wt% TiO_2-CNT on aluminum panels.

4. Conclusions

In summary, this study prepared TiO_2-decorated MWCNT hybrids and dispersed them into a PAA matrix for strong radiative cooling coatings. The TiO_2 nanoparticles were in situ grown on the CNTs, forming a rough surface that can produce asperity contacts and enhance the interaction of CNTs with PAA. Consequently, the composite with a small fraction of the hybrid loading (0.1 wt%) exhibited a 24.8% higher strength than the pure PAA film (from 13.7 MPa to 17.1 MPa). In comparison to previous studies—such as the work by Prashantha et al. [22], who reported a 17.73% increase in the tensile strength of polypropylene (PP) with the addition of 1 wt% MWCNTs, and that by Safadi et al. [23], who achieved a 25.64% enhancement in polystyrene (PS) with the same loading—this composite, based on CNTs' exceptional thermal conductivity and record-high infrared emissivity, significantly enhances heat dissipation, thereby achieving a remarkable cooling effect at a substantially lower filler concentration. The optimized 0.1 wt% composite coating demonstrates an equilibrium temperature cooling efficiency of 13.15% compared with the bare Al substrate, which is considerable when compared to the results reported by Suryawanshi et al. [24], where a 10.34% equilibrium temperature cooling efficiency was obtained using a higher CNT loading of 0.4 wt%. Such a composite might have potential for thermal management, since it combines enhanced strength and an excellent cooling effect based on the TiO_2-CNTs hybrid fillers.

Author Contributions: Conceptualization, Y.M. and X.J.; formal analysis, J.W., Y.L. and D.L.; investigation, J.W. and Y.M.; writing—original draft preparation, J.W., Y.M. and X.J.; writing—review and editing, X.J.; supervision, Y.M. and X.J.; project administration, Y.M. and X.J.; funding acquisition, Y.M. and X.J. All authors have read and agreed to the published version of the manuscript.

Funding: This work was supported by the research fund of State Grid Tangshan Power Supply Company (B3010322000Y).

Institutional Review Board Statement: Not applicable.

Informed Consent Statement: Not applicable.

Data Availability Statement: Data are included in the article.

Conflicts of Interest: Authors Yong Liu, Dapeng Liu, Yong Mu were employed by Tangshan Power Supply Company, State Grid Jibei Electric Power Co., Ltd. The remaining authors declare that the research was conducted in the absence of any commercial or financial relationships that could be construed as a potential conflict of interest.

References

1. Li, X.; Song, W.; Wang, Q.; Li, H.; Ding, X.; Liu, S. Optimizing cooling electronic chips at high altitude with consideration of solar radiation. *Int. J. Therm. Sci.* **2023**, *183*, 107879. [CrossRef]
2. Ren, Y.; Wang, H.; Xing, B.; Qu, W.; Li, Z.; Ren, J.; Zhang, J.; Zhao, J. Preparation and performance evaluation of graphene-based waterborne thermal conductive coatings. *Surf. Coat. Technol.* **2024**, *478*, 130422. [CrossRef]
3. Sun, K.; Xie, Y.; Fang, X.; Li, H.; Lai, Q.; Tan, J. An experimental study of spectral radiative properties of multi-walled carbon nanotube coating for heat dissipation. *Case Stud. Therm. Eng.* **2023**, *41*, 102660–102670. [CrossRef]
4. Li, X.; Xie, Z.; Chen, B.; Cai, L.; Zhao, D.; Du, K.; Qiu, M. Transparent radiative cooler with high thermal conductivity for heat dissipation in electronic devices. *Cell Rep. Phys. Sci.* **2025**, *6*, 102505. [CrossRef]
5. Mandal, J.; Fu, Y.; Overvig, A.C.; Jia, M.; Sun, K.; Shi, N.N.; Zhou, H.; Xiao, X.; Yu, N.; Yang, Y. Hierarchically porous polymer coatings for highly efficient passive daytime radiative cooling. *Science* **2018**, *362*, 315–319. [CrossRef] [PubMed]
6. Li, T.; Zhai, Y.; He, S.; Gan, W.; Wei, Z.; Heidarinejad, M.; Dalgo, D.; Mi, R.; Zhao, X.; Song, J.; et al. A radiative cooling structural material. *Science* **2019**, *364*, 760–763. [CrossRef]
7. Zeng, S.; Pian, S.; Su, M.; Wang, Z.; Wu, M.; Liu, X.; Chen, M.; Xiang, Y.; Wu, J.; Zhang, M.; et al. Hierarchical-morphology metafabric for scalable passive daytime radiative cooling. *Science* **2021**, *373*, 692–696. [CrossRef]
8. Zhou, L.; Song, H.; Liang, J.; Singer, M.; Zhou, M.; Stegenburgs, E.; Zhang, N.; Xu, C.; Ng, T.; Yu, Z.; et al. A polydimethylsiloxane-coated metal structure for all-day radiative cooling. *Nat. Sustain.* **2019**, *2*, 718–724. [CrossRef]
9. Li, D.; Liu, X.; Li, W.; Lin, Z.; Zhu, B.; Li, Z.; Li, J.; Li, B.; Fan, S.; Xie, J.; et al. Scalable and hierarchically designed polymer film as a selective thermal emitter for high-performance all-day radiative cooling. *Nat. Nanotechnol.* **2021**, *16*, 153–158. [CrossRef]
10. Bao, H.; Yan, C.; Wang, B.; Fang, X.; Zhao, C.Y.; Ruan, X. Double-layer nanoparticle-based coatings for efficient terrestrial radiative cooling. *Sol. Energy Mater. Sol. Cells* **2017**, *168*, 78–84. [CrossRef]
11. Cheng, Z.; Shuai, Y.; Gong, D.; Wang, F.; Liang, H.; Li, G. Optical properties and cooling performance analyses of single-layer radiative cooling coating with mixture of TiO_2 particles and SiO_2 particles. *Sci. China Technol. Sci.* **2020**, *64*, 1017–1029. [CrossRef]
12. Eyassu, T.; Hsiao, T.J.; Henderson, K.; Kim, T.; Lin, C.T. Molecular cooling fan: Factors for optimization of heat dissipation devices and applications. *Ind. Eng. Chem. Res.* **2014**, *53*, 19550–19558. [CrossRef]
13. Pakzad, E.; Ranjbar, Z.; Ghahari, M. Synthesized of octahedral cupper chromite spinel for spectrally selective absorber (SSA) coatings. *Prog. Org. Coat.* **2019**, *132*, 21–28. [CrossRef]
14. Yang, Z.P.; Ci, L.; Bur, J.A.; Lin, S.-Y.; Ajayan, P.M. Experimental observation of an extremely dark material made by a low-density nanotube array. *Nano Lett.* **2008**, *8*, 446–451. [CrossRef]
15. Mizuno, K.; Ishii, J.; Kishida, H.; Hayamizu, Y.; Yasuda, S.; Futaba, D.N.; Yumura, M.; Hata, K. A black body absorber from vertically aligned single-walled carbon nanotubes. *Proc. Natl. Acad. Sci. USA* **2009**, *106*, 6044–6047. [CrossRef] [PubMed]
16. Qi, X.; Xu, H.; Wang, X.Q.; Ma, W.G.; Qiu, C.; An, M.; Zhang, G.; Wang, F.; Zhang, X.; Bermak, A. Effective surface emissivity and heat dissipation among integrated bamboo-like super-black vertical carbon nanotube array electrodes in silicon via holes. *Carbon* **2020**, *158*, 846–856. [CrossRef]
17. Liu, X.; Tang, Y.; Liu, Y.; Cao, Z.; Wang, R.; Wang, B.; Wang, B. Enhanced low-temperature radiative cooling and marine durability of stainless steel with a novel multi-layered composite coating. *Surf. Interfaces* **2025**, *62*, 106260. [CrossRef]
18. Yu, Z.; Wang, F.; He, W.; Wang, Y.; Dai, B.; Zhang, X. Phase-change material- integrated dual-mode thermal management janus films with enhanced radiative cooling and solar heating. *ACS Appl. Polym. Mater.* **2025**, *7*, 3555–3563. [CrossRef]
19. Ji, R.; Wang, S.; Zhao, X.; Zhang, J.; Zou, Y.; Chen, G.; Wang, Y.; Huang, Y.; Ouyang, J.; Jia, D.; et al. TiO_2-BN/CNTs coating with radiative cooling and reduced friction. *Chem. Eng. J.* **2024**, *493*, 152802. [CrossRef]
20. Mastai, Y.; Diamant, Y.; Aruna, S.T.; Zaban, A. TiO_2 nanocrystalline pigmented polyethylene foils for radiative cooling applications: Synthesis and characterization. *Langmuir* **2001**, *17*, 7118–7123. [CrossRef]
21. Mishra, B.R.; Sundaram, S.; Sasihithlu, K. Cooling performance of TiO2-based radiative cooling coating in tropical conditions. *ACS Omega* **2024**, *9*, 49494–49502. [CrossRef] [PubMed]
22. Prashantha, K.; Soulestin, J.; Lacrampe, M.F.; Krawczak, P.; Dupin, G.; Claes, M. Masterbatch-based multi-walled carbon nanotube filled polypropylene nanocomposites: Assessment of rheological and mechanical properties. *Compos. Sci. Technol.* **2009**, *69*, 1756–1763. [CrossRef]
23. Safadi, B.; Andrews, R.; Grulke, E.A. Multiwalled carbon nanotube polymer composites: Synthesis and characterization of thin films. *J. Appl. Polym. Sci.* **2002**, *84*, 2660–2669. [CrossRef]
24. Suryawanshi, C.N.; Lin, C.T. Radiative cooling: Lattice quantization and surface emissivity in thin coatings. *ACS Appl. Mater. Interfaces* **2009**, *1*, 1334–1338. [CrossRef]
25. Yamabe, H. Stabilization of the polymer-metal interface. *Prog. Org. Coat.* **1996**, *28*, 9–15. [CrossRef]
26. Sun, B.; Liu, Q.; Gao, Y.; Han, L.; Zhang, R.; Zhang, C.; Jia, X. Preparation of carbon nanotube-reinforced polyethylene nanocomposites with better anti-scaling and corrosion-resistant properties. *Ind. Chem. Mater.* **2024**, *2*, 154–164. [CrossRef]
27. *GB/T 9286-2021*; Paints and Varnishes—Cross-Cut Test. National Standard of the People's Republic of China: Beijing, China, 2021.

28. Sinani, V.A.; Gheith, M.K.; Yaroslavov, A.A.; Rakhnyanskaya, A.A.; Sun, K.; Mamedov, A.A.; Wicksted, J.P.; Kotov, N.A. Aqueous dispersions of single-wall and multiwall carbon nanotubes with designed amphiphilic polycations. *J. Am. Chem. Soc.* **2005**, *127*, 3463–3472. [CrossRef]
29. Gao, Y.; Li, L.; Tan, P.; Liu, L.; Zhang, Z. Application of Raman spectroscopy in carbon nanotube-based polymer composites. *Chin. Sci. Bull.* **2010**, *55*, 3978–3988. [CrossRef]
30. Kotsilkova, R.; Angelova, P.; Batakliev, T.; Angelov, V.; Di Maio, R.; Silvestre, C. Study on aging and recover of poly (lactic) acid composite films with graphene and carbon nanotubes produced by solution blending and extrusion. *Coatings* **2019**, *9*, 359. [CrossRef]
31. Cui, C.; Qian, W.; Zhao, M.; Xu, G.; Nie, J.; Jia, X.; Wei, F. High-yield synthesis of nanohybrid shish-kebab polyethylene-carbon nanotube structure. *Chin. J. Chem. Eng.* **2013**, *21*, 37–43. [CrossRef]
32. Cui, C.; Qian, W.; Zhao, M.; Ding, F.; Jia, X.; Wei, F. High strength composites using interlocking carbon nanotubes in a polyimide matrix. *Carbon* **2013**, *60*, 102–108. [CrossRef]

Disclaimer/Publisher's Note: The statements, opinions and data contained in all publications are solely those of the individual author(s) and contributor(s) and not of MDPI and/or the editor(s). MDPI and/or the editor(s) disclaim responsibility for any injury to people or property resulting from any ideas, methods, instructions or products referred to in the content.